

Path Planning for Emergency Response and Rescue Vessels in Inland Rivers by Improved Artificial Potential Field Algorithms

Jingyu Yu^{1,2,3}, Qingyu Shi¹, Wei Lin⁴, Jingfeng Wang^{1,2,3} and Yuxue Pu^{1,2,3}

Received: 06 August 2024 / Accepted: 26 January 2025

© Harbin Engineering University and Springer-Verlag GmbH Germany, part of Springer Nature 2025

Abstract

Frequent flood disasters caused by climate change may lead to tremendous economic and human losses along inland waterways. Emergency response and rescue vessels (ERRVs) play an essential role in minimizing losses and protecting lives and property. However, the path planning of ERRVs has mainly depended on expert experiences instead of rational decision making. This paper proposes an improved artificial potential field (APF) algorithm to optimize the shortest path for ERRVs in the rescue process. To verify the feasibility of the proposed model, eight tests were carried out in two water areas of the Yangtze River. The results showed that the improved APF algorithm was efficient with fewer iterations and that the response time of path planning was reduced to around eight seconds. The improved APF algorithm performed better in the ERRV's goal achievement, compared with the traditional algorithm. The path planning method for ERRVs proposed in this paper has theoretical and practical value in flood relief. It can be applied in the emergency management of ERRVs to accelerate flood management efficiency and improve capacity to prevent, mitigate, and relieve flood disasters.

Keywords Emergency response and rescue vessels (ERRVs); Artificial potential field (APF) algorithm; Path planning; Emergency management; Inland rivers

1 Introduction

Inland waterways are the origin of civilization. Even in modern society, people still rely heavily on inland waterways for their livelihoods. Populations are often concentrated in inland river basins such as the Amazon, Nile, Yangtze, Pearl, Rhine, and Mississippi Rivers. At the end of 2020, the navigable mileage of China's inland water-

ways was 127 700 kilometers, ranking first in the world (Liu, 2021). In China, the main stream of the Yangtze River is more than 6 300 kilometers long, with a basin area of about 1.8 million square kilometers, accounting for roughly 18.8% of China's land area. The population of the Yangtze River basin is over 460 million, about 33% of China's population. The gross output of the Yangtze River basin makes up around 34% of national GDP (Ministry of Ecology and Environment of China, 2022). However, frequent inland flood disasters result in enormous economic losses, damage to cultural heritage, environmental impairment, and loss of life (Borowska-Stefańska et al., 2023). Between 2000 and 2019 there were 3 254 floods globally, affecting 1.65 billion people (Mizutori and Guha-Sapir, 2020). It is estimated that between 1870 and 2016, floods affected on average 0.03% of the European population per year, causing damage equivalent to 0.08%–0.09% of GDP (Paprotny et al., 2018). In comparison with developed countries, developing countries are more likely to suffer from human casualties and economic losses due to their weak economic base and imperfect flood prevention and control systems. The catastrophic floods in India in June 2013 led to more than 5 000 deaths (Hirabayashi et al., 2013). It is estimated that there are up to 20 000 deaths and over 25 million people displaced by floods worldwide each year (Kellens et al., 2013).

Article Highlights

- An improved artificial potential field (APF) algorithm is proposed to optimize the shortest path for ERRVs in the rescue process.
- A naturally smooth path is achieved by varying the gradient of the repulsive potential field without taking additional curve fitting.
- With the improved APF algorithm, the path planning for an area of 4 000 000 units could be completed in eight seconds.

✉ Qingyu Shi
ching.s@foxmail.com

¹ College of Civil Engineering, Hefei University of Technology, Hefei 230009, China

² Engineering Research Center of Low-carbon Technology and Equipment for Cement-based Materials, Ministry of Education, Hefei University of Technology, Hefei 230009, China

³ Anhui Key Laboratory of Civil Engineering Structures and Materials, Hefei University of Technology, Hefei 230009, China

⁴ Anhui Tendering Group, Hefei 230051, China

Floods accounted for 38.4% of global natural disasters in 2017 (Li et al., 2019). In responding to floods, it is important to both recover from the disaster and establish a local flood protection system (Borowska-Stefańska et al., 2023). As an important part of the local flood protection system, inland waterway rescues are necessary and urgently needed to minimize injuries, deaths, and property damage. Emergency rescue vessels (ERRVs) are an important component of national emergency and security systems. ERRVs provide medical after-care facilities and mechanical recovery devices for timely salvage and rescue. They are also equipped with engineering machinery for conducting disaster relief work such as piling, closing breach, riprapping, and dredging. These vehicles are often large and heavy with abundant equipment and machines, and cannot sail through narrow inland waterways. Traditional scheduling programs that rely on expert knowledge and experience may not succeed in reaching rescue points within complex inland water areas. Path planning for ERRVs is necessary to avoid stranding in complex inland waterways leading to failure of rescue operations, and better ERRV path planning is critical to improve the efficiency of the rescue. Therefore, quick planning of an optimal route in complex and changing inland waterways is a key technical problem that needs to be solved urgently.

While path planning studies are popular, most of them are focused on overland vehicles. There are few studies for path planning of ERRVs, especially for inland rivers. In this paper, an improved artificial potential field (APF) algorithm is developed to optimize the paths of inland ERRVs with short response times and sailing distances. A smoothing strategy based on the improved repulsive potential field is also proposed to simulate the dynamics characteristic of inland ERRVs, including rapid speed and under-driven navigation. The Yangtze River basin was selected as the study area and eight tests were conducted based on its conditions to verify the proposed path planning model.

2 Literature review

Most current studies emphasize vessel scheduling for different rescue scenarios (Ma et al., 2023), while vessel-specific path planning has rarely been investigated (Xiong et al., 2020). Due to the intricate changes of inland flood disasters, a quick response under complex conditions is required. Fast and accurate path planning is key to increasing rescue efficiency of ERRVs and for human and property protection (Zhang et al., 2021). Path planning and decision making for inland ERRVs are inherently complex tasks, influenced by a multitude of factors such as waterline, wind speed, sail speed, and disaster losses. Hence, path planning for inland ERRVs is a typical non-deterministic polynomial (NP) hard problem (Pinedo, 2022). To

solve such a problem, there are three types of algorithms: intelligent algorithms, sampling-based algorithms, and traditional algorithms (Table 1).

Intelligent algorithm is a general term for bionic algorithms and machine learning algorithms. In recent years, intelligent algorithms have been widely used to improve the performance of computer-assisted decision-making processes. Most intelligent algorithms including genetic algorithms (GA) (Pehlivanoglu and Pehlivanoğlu, 2021), neural network algorithms (Sung et al., 2021), metaheuristic optimization algorithms (Khan et al., 2020), and deep reinforcement learning (DRL) algorithms (Lan et al., 2024) have been applied in path planning for different vehicles and vessels. For specific vessel path planning, the complexity of obstacle situations makes it difficult to adapt a single intelligent algorithm to simulate the environment. Therefore, hybrid algorithms are commonly used (Wang et al., 2021b). Li et al. (2021) proposed autonomous collision avoidance path planning by combining a DRL algorithm with an APF algorithm. Lyridis (2021) improved an ant colony optimizer (ACO) with Fuzzy Logic to address the multi-objective problem of unmanned surface vessel (USV) path planning and obstacle avoidance. However, after making such improvements, the intelligent algorithms took longer to solve path planning problems (Gan et al., 2022), which is not conducive to quick responses to dynamic and complex floor disaster relief works.

The rapidly random tree (RRT) algorithm is the most widely used sampling-based algorithm for path planning. It is able to quickly find a satisfactory path with simple obstacle modeling (Liao et al., 2021). However, under sampling-based algorithms, there are redundant points in planning paths (LaValle, 1998), leading to an unsmooth path. Therefore, many studies adopting sampling-based algorithms have focused on how to smooth the paths. Chi et al. (2022) utilized the generalized Voronoi diagram (GVD) feature matrix to fuse the nodes to plan a smooth path for mobile robots. After generating the path with the RRT algorithm, Cao et al. (2022) used the three-order B-spline curve to obtain a smooth path. Although there are plentiful similar studies, smoothing does not often work well for RRT algorithms, especially when the path is long (Yu et al., 2024; Ye et al., 2023; Tu et al., 2024). Additionally, sampling-based algorithms suffer from high randomness and are non-optimal (Cao et al., 2022).

An artificial potential field (APF) algorithm is often used in vessel path planning for simplicity and real-time performance (Gan et al., 2022). This elegant algorithm is widely used in unmanned aerial vehicles (Zhou and Kong, 2022), vessels (Lyu and Yin, 2019), and robots (Rodríguez-Guerra et al., 2023). Since the original APF algorithm is prone to fall into local minimum, numerous improvements have been made in recent studies (Ni et al., 2021; Liu et al., 2024a). Liu et al. (2024b) introduced dynamic perturbation

Table 1 Summary of path planning studies

Citation	Algorithm	Algorithm type	Smoothing strategy	Areas of application
Pehlivanoglu et al. (2021)	Genetic algorithm (GA), ant colony optimizer (ACO) algorithm	Intelligent algorithm	Bezier curves	Unmanned aerial vehicles (UAV)
Sung et al. (2021)	Neural network algorithm	Intelligent algorithm	Quadratic program (QP)	Automated vehicles
Khan et al. (2020)	Metaheuristic optimization algorithm	Intelligent algorithm	–	Mobile-manipulator
Lan et al. (2024)	Deep reinforcement learning (DRL) algorithm	Intelligent algorithm	–	Underwater gliders
Li et al. (2021)	DRL algorithm, artificial potential field (APF) algorithm	Intelligent algorithm	B-spline curve	Unmanned surface vessels (USV)
Lyridis et al. (2021)	ACO algorithm	Intelligent algorithm	–	USV
Wang et al. (2021a)	Particle swarm optimization (PSO) algorithm, APF algorithm	Intelligent algorithm	–	USV
Chi et al. (2022)	Rapidly exploring random tree variants (RRTs) algorithm	Sampling-based algorithm	Generalized Voronoi diagram (GVD)	Mobile robots
Cao et al. (2022)	Rapidly exploring random tree (RRT) algorithm	Sampling-based algorithm	B-spline curve	Vessels
Ye et al. (2023)	RRT algorithm	Sampling-based algorithm	–	Mobile robots
Yu et al. (2024)	RRT algorithm	Sampling-based algorithm	Three-order B-spline curve	Autonomous vehicles
Tu et al. (2024)	RRT algorithm	Sampling-based algorithm	Collision detections	Indoor environments
Liu et al. (2024c)	Adaptive Step Size Informed-RRT* Algorithm	Sampling-based algorithm	–	Vessels
Fazlollahtabar (2018)	Composed sub-gradient algorithm	Traditional algorithm	–	Automated guided vehicles
Lyu and Yin (2019)	APF algorithm	Traditional algorithm	–	USV
Ni et al. (2021)	APF algorithm	Traditional algorithm	–	USV, marine autonomous surface ships (MASS)
Sang et al. (2021)	APF algorithm, A* algorithm	Traditional algorithm	–	USV
Gan et al. (2022)	APF algorithm	Traditional algorithm	–	Vessels
Rao et al. (2023)	APF algorithm, A* algorithm	Traditional algorithm	–	UAV
Zhou and Kong (2022)	APF algorithm	Traditional algorithm	–	UAV
Rodríguez-Guerra et al. (2023)	APF algorithm	Traditional algorithm	–	Robots
Liu et al. (2024)	APF algorithm	Traditional algorithm	–	Clustered UAVs
Zhai et al. (2024)	Sparse A* Algorithm	Traditional algorithm	–	Vessels
Liu et al. (2024)	APF algorithm	Traditional algorithm	B-spline curves	UAV

to address the local minimum problem. The A* algorithm is also used to combine with the APF algorithm to enhance the global search capability (Sang et al., 2021; Rao et al., 2023). The paths generated by this integrated algorithm are smooth and generally no additional smoothing strategies are required.

To sum up, intelligent algorithms are inadequate for path planning of inland ERRVs, because flood disasters that

occur in rivers often change rapidly. There might be limited time to learn the data and run the whole program of intelligent algorithms. Moreover, inland rivers are not straight lines, but have numerous obstacles under water. The complex environment of inland water areas makes it difficult to generate smooth paths by sampling-based algorithms. The planning of a suitable path for ERRVs within an acceptable time plays an important role in flood rescue projects

(Ozkan et al., 2019). To fill this gap, it seems that the APF algorithm is the best option for path planning of ERRVs in complex inland waters. Therefore, this paper proposed an improved APF algorithm by avoiding local minimum problems and the proposed method was applied to solve path planning problems for inland ERRVs.

3 Methodology

3.1 Traditional APF

The artificial potential field (APF) is a virtual force method proposed by Khatib (1985). APF sets the gravitational field at the destination and the repulsive field at the obstacles. The algorithm ensures the objects approach the destination while avoiding obstacles. To solve path planning of inland ERRVs, the original position of the ERRV is expressed as $X = (x, y)$. The position of the goal of the ERRV is represented as $X_t = (x_t, y_t)$, and the position of the obstacle from the original position to the goal is represented as $X_o = (x_o, y_o)$. The gravitational potential field function is defined as:

$$U_{att} = \frac{1}{2} \lambda R^2 \tag{1}$$

where λ is gravitational parameter, and R the distances between the original position of the ERRV and the goal, which can be defined as:

$$R = \|X - X_t\| = \sqrt{(x - x_t)^2 + (y - y_t)^2} \tag{2}$$

The goal position exerts a gravitational force on the ERRV. The magnitude is the negative gradient of the gravitational potential field function, such that:

$$F_a = -\text{grad}(U_{att}) = -\lambda R \tag{3}$$

The repulsive potential field function is defined as:

$$U_r = \begin{cases} \frac{1}{2} \mu \left(\frac{1}{r} - \frac{1}{\alpha_o} \right)^2, & r \leq \alpha_o \\ 0, & r > \alpha_o \end{cases} \tag{4}$$

where U_r is the repulsive force field generated by the obstacle on the ERRV, μ the repulsive force parameter, and α_o the radius of influence of the obstacle. When the ERRV was out of the radius (α_o), the obstacle had no repulsive influence on the ERRV. r is the distances between the current state of the vessel and the obstacle, which can be defined as:

$$r = \|X - X_o\| = \sqrt{(x - x_o)^2 + (y - y_o)^2} \tag{5}$$

The obstacle exerts a repulsive force on the ERRV as:

$$F_r = -\text{grad}(U_r) = \begin{cases} \mu \left(\frac{1}{r} - \frac{1}{\alpha_o} \right) \frac{1}{r^2} \frac{\partial \alpha}{\partial X}, & r \leq \alpha_o \\ 0, & r > \alpha_o \end{cases} \tag{6}$$

The combined force on the ERRV is:

$$F = F_a + \sum_{i=1}^n F_r^i \tag{7}$$

where i is the number of obstacles and F_r^i the repulsive force of the i^{th} obstacle on the ERRV.

The traditional APF method benefits from concise modeling, high efficiency, and rapid speed of convergence, which can satisfy the local dynamic obstacle avoidance of the ERRV. Nevertheless, the traditional APF method has planning failures in some cases. For example, when the distance between the goal and the obstacle is close, the gravitational force tends to reduce and the repulsive force increases. The path planning could fail as the combined forces of the ERRV are directed away from the goal (see Figure 1). If the combined force on the ERRV is 0 or if the gravitational and repulsive forces are co-linear (see Figure 2), the vessel will appear to stall or wander in a localized area. Thus, it falls into a local minimum.

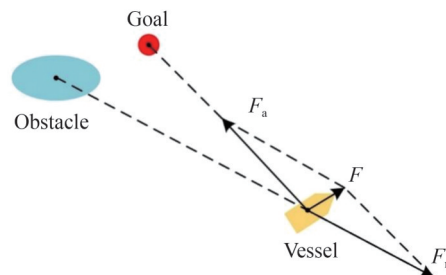


Figure 1 Failure case of APF method (unable to reach the goal)

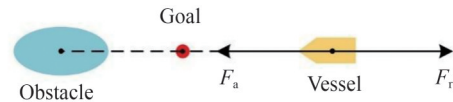


Figure 2 Failure case of APF method (stuck in a local minimum)

3.2 Improved APF for inland river ERRVs

Compared to the navigable environment at sea, inland waterways are narrow and shallow (Bolbot et al., 2020). Flood disasters occurring in inland water areas often create an even more complex and dangerous environment, such as converging waters, curved waters, and vortexes. (Roeleven et al., 1995). The poor natural conditions of inland waters make the passage of ERRVs difficult. To address

the path planning failures of traditional APF algorithms, a series of improvements can be made, including repulsive potential field correcting, virtual obstacles setting, and path smoothing.

3.2.1 Repulsive potential field correcting

A correction of a repulsive potential field function is amended as U_{rg} , expressed as Equation 8. A parameter β included in the corrected repulsive potential field aims to fix the direction of the combined force biased towards the destination. The value of β is between 0 and 1.

$$U_{rg} = \begin{cases} \frac{1}{2} \mu \left(\frac{1}{r} - \frac{1}{\alpha_0} \right)^2 R^\beta, & r \leq \alpha_0 \\ 0, & r > \alpha_0 \end{cases} \quad (8)$$

After the improvement of the APF algorithm, additional force directed at the goal is applied. The distance R between the original position of the ERRV and its goal position is taken as the influence factor. The negative gradient of the repulsive potential field function on the ERRV is expressed as:

$$F_{rg} = -\text{grad}(U_{rg}) = \begin{cases} F_{rg1} + F_{rg2}, & r \leq \alpha_0 \\ 0, & r > \alpha_0 \end{cases} \quad (9)$$

$$F_{rg1} = \mu \left(\frac{1}{r} - \frac{1}{\alpha_0} \right) \frac{1}{r^2} \frac{\partial \alpha}{\partial X} R^\beta \quad (10)$$

$$|F_{rg1}| = \mu \left(\frac{1}{r} - \frac{1}{\alpha_0} \right) \frac{1}{r^2} R^\beta \quad (11)$$

$$F_{rg2} = -\frac{\beta}{2} \mu \left(\frac{1}{r} - \frac{1}{\alpha_0} \right)^2 R^{\beta-1} \frac{\partial R}{\partial X} \quad (12)$$

$$|F_{rg2}| = \frac{\beta}{2} \mu \left(\frac{1}{r} - \frac{1}{\alpha_0} \right)^2 R^{\beta-1} \quad (13)$$

From Equations 11 and 13, only when the value of β is between 0 and 1, as the value of R decreases, the force F_{rg2} pointing toward the goal becomes larger and the force F_{rg1} back away from the obstacle becomes small. In this case, the direction of the combined force on the ERRV is constantly corrected toward the goal, and thus it will continually move to the goal. The distinct angle θ of bias toward the goal being marked in Figure 3. The value of angle θ is expressed as Equation 14. The corrected repulsive field decreases due to proximity to the goal, which visually explains the role of F_{rg2} (as shown in Figure 4).

$$\theta = \arccos \left(\frac{|F|^2 + |F_g|^2 - |F_{rg2}|^2}{2|F| \cdot |F_g|} \right) \quad (14)$$

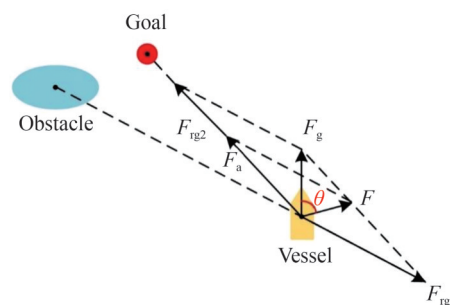
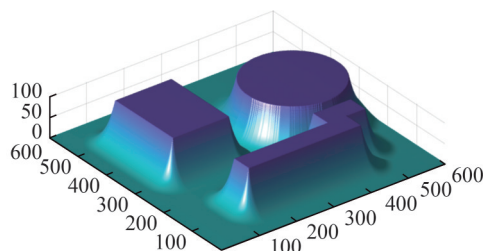
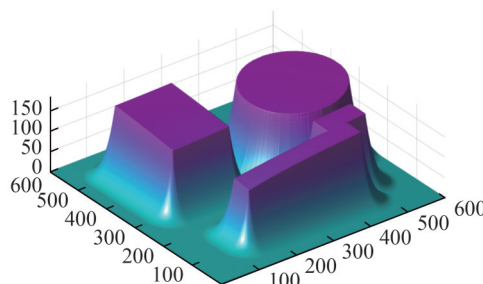


Figure 3 Force diagram after modification of the repulsive force



(a) Initial repulsive potential field



(b) Corrected repulsive potential field

Figure 4 Example of repulsive potential field correcting

3.2.2 Virtual obstacles setting

Large obstacles or U-shaped obstacles may cause local minimum issues, as the combined force could become 0 before reaching the goal. Virtual obstacles are set to address this flaw. The specific flow of the improved algorithm is shown in Figure 5. When the combined force of the ERRV is 0 in path planning, it is determined whether the goal is reached. If not, it is concluded that it is in a local minimum and the virtual obstacle will be set. The virtual obstacle is a solid circle with radius ρ and center's coordinates $(x + m, y + n)$, denoted as $O_v(x + m, y + n, \rho)$. Coordinates (x, y) is the coordinate of the local minimum point in this path planning. Virtual obstacles at (x, y) will fail to resolve the co-linear situation. Therefore, the virtual obstacle is set near the local minimum point by randomized correction parameters m and n . The vessel will not be stuck in this local minimum further, as shown in Figure 6(b). With this virtual obstacle in place, the path is re-planned and the combined force detection mentioned above is repeated. If a local minimum issue occurs again, new virtual obstacles will be set until the goal is reached.

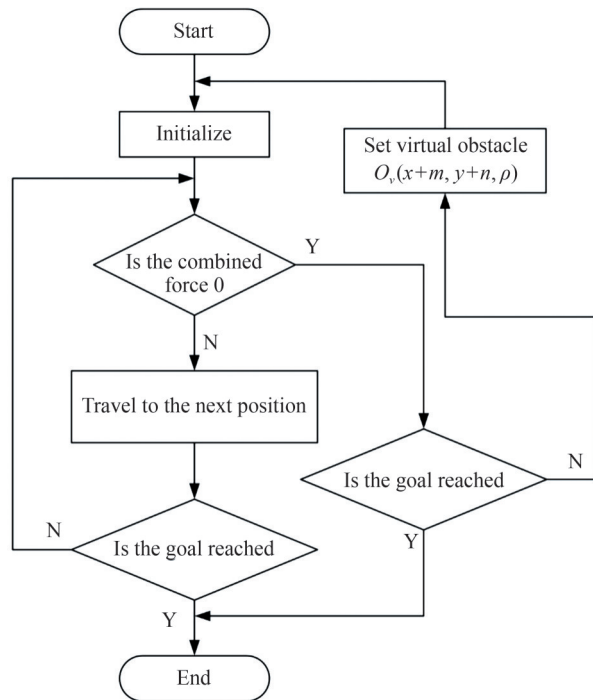


Figure 5 Flowchart of path planning for the introduction of virtual obstacles

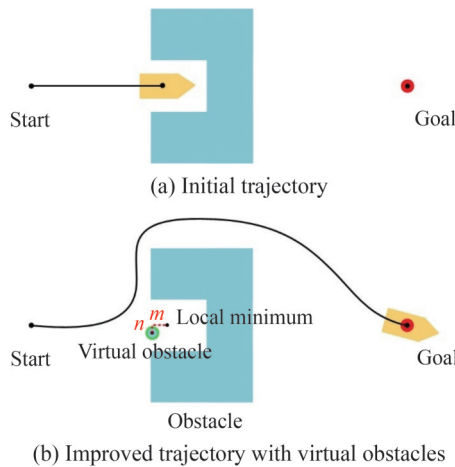


Figure 6 Example of trajectories with and without virtual obstacles

3.2.3 Path smoothing

Considering the complex inland water environment and traveling characteristics of ERRVs (i.e., a certain turning radius, heavy weight, and high inertia), a smooth path is desired in the planning. Previous path smoothing strategies frequently used cubic spline (Li et al., 2021); however, cubic spline fails to guarantee the smoothness of the entire curve, and additional nodes to avoid local smoothness would significantly reduce the efficiency (Silverman, 1985). A smoothing strategy for ERRVs is thus developed by amending the repulsive potential field function to make the transit smoother. On the basis of Equation 8, the repulsive potential field function is modified as:

$$U_{rs} = \begin{cases} \frac{n\mu}{2} \left(\frac{1}{r/n + 1} - \frac{1}{\alpha_0} \right)^2 R^\beta, & r \leq \alpha_0/n + 1 \\ 0, & r > \alpha_0/n + 1 \end{cases} \quad (15)$$

n : correction factor for the distance between the ERRV and the obstacle, $n > 1$.

The repulsive force in the direction of the line joining the ERRV and the obstacle in the range $r \leq \alpha_0/n + 1$ is as follows:

$$|F_{rs1}| = \left(\frac{1}{r/n + 1} - \frac{1}{\alpha_0} \right) \frac{\mu R^\beta}{(r/n + 1)^2} \quad (16)$$

The repulsive effect of the goal on the ERRV (F_{rs2}) is not taken into account. The magnitude of the repulsive force varies more smoothly with the improvement. n determines how the repulsive forces vary smoothly with r . The repulsive force on the ERRV is similar to the original with smaller n , and change more smoothly with larger n (as shown in Figure 7).

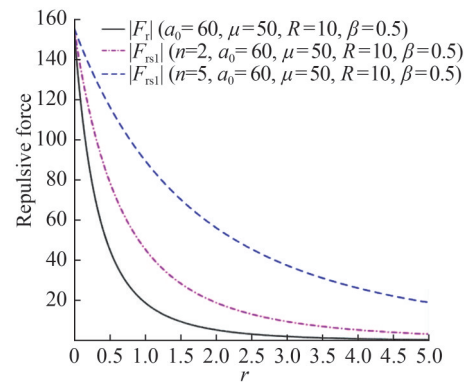


Figure 7 Comparison of repulsive force magnitude

With parameters other than n determined, the repulsive force on ERRV is compared as the distance r from the obstacle varies. Traditional. The AFP algorithm has excessive repulsion variation near obstacles, as shown in Figure 7. In large maps, even a tiny increase in α_0 could result in significant improvements. This leads to inevitable sharp corners in the path (Figure 8(a)). With the improved APF algorithm, the trajectory obtained is smooth without sharp corners, as shown in Figure 8b. The exact value of n is related to numerous factors, such as the map size, the complexity of the map, etc. It is recommended to refer to Equation 16 for the approximate value of n :

$$n = \frac{\text{Map} - \text{Size}}{20 \times \text{Step} - \text{Size}} \quad (17)$$

The improved APF algorithm is given in Algorithm 1.

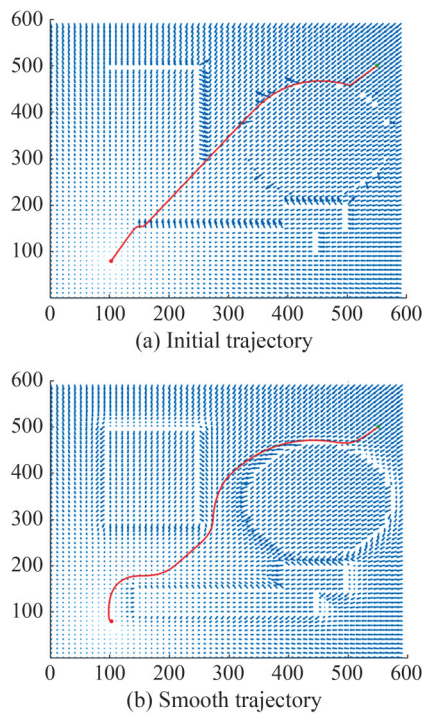


Figure 8 Example of trajectories by initial and smoothing strategy

Algorithm 1: Improved APF algorithm

Input: the coordinates x_0 of the start, the coordinates x_g of the goal, the information M on the map

Output: the planned path L

```

1  for iterations  $i=0 \rightarrow$  Maximum iterations do
2      Calculate the gravitational potential  $U_{att}$  using (1);
3      Calculate the repulsive potential  $U_{rs}$  using (15);
4      Calculate the combined force  $F_i$  at  $x_i$ ;
5      if  $F_i = 0$  then
6          if  $x_0 = x_g$  then
7              break;
8          else
7          Set a virtual obstacle  $O_v(x + m, y + n, \rho)$ ;
8           $i \leftarrow 0$ ;
9          end if
10     else
11     Update coordinates to  $x_{i+1}$ ;
12     end if
13     Record the coordinates of each step taken as  $[x_0, \dots, x_{i+1}]$ ;
13  end for
14  Generate the planned path  $L$  from  $[x_0, \dots, x_{i+1}]$ ;
15  Output  $L$ ;
```

4 Case study

The inland river ERRV in Anhui Province was chosen

as a case study to verify the proposed path planning method. The case study ERRV belongs to modernized multifunctional vessels, as shown in Figure 9. The vessel was equipped with plenty of engineering machines, including a crane with a capacity of 120 tons, a packing machine, and trebuchet to support flood rescue works. The ERRV thus has large loads that make it difficult to sail in the complex inland waterways. Considering the urgency of flood rescue efforts, a rapid response speed is required and a smooth path for the ERRV. Therefore, planning algorithms are needed to consider the typical characteristics of the ERRV (see Table 2).



Figure 9 An inland river ERRV

Table 2 Parameters of a typical inland river ERRV

Length	Width (m)	Speed (km/h)	Moulded depth (m)	Mileage (km)	Cargo capacity (t)
54.50	18	13	3.6	1 000	120

Anhui, a key province in the lower reaches of the Yangtze River, collaborates with Shanghai, Suzhou, and Zhejiang to create a world-class port cluster in the Yangtze River Delta. In 2023, the mileage of high-grade waterways in Anhui Province with four or more levels exceeded 2 360 kilometers, ranking third in China (Fan and Xu, 2023). With such long and complex waterways, Anhui often suffers from flood disasters. The path planning of the ERRV is important to secure life and property safety in Anhui. In the current study, two Yangtze River areas in Anhui Province were selected as experimental scenarios for the case study, using MATLAB R2022b on a personal computer with 11th Gen Intel® Core™ i7 and 16 GB RAM.

The land cover data used in the case study was obtained from the open database GlobeLand30 (National Geomatics Center of China, 2024) and was converted to binary data on the river channel (see Figure 10). As ERRV is used as an emergency rescue, a service range of 10 to 15 km is appropriate based on an arrival time of 45 minutes. Two typical areas were selected, represented as Area 1 and Area 2. Area 1 was a 20 km square area (center coordinates 118°20'21.008"E, 31°28'13.473"N) and Area 2 was a 15 km square area (center coordinates 117°27'52.233"E, 30°43'23.276"N). Both areas were pre-treated with 2 000 units of length and width. Eight tests were carried out in

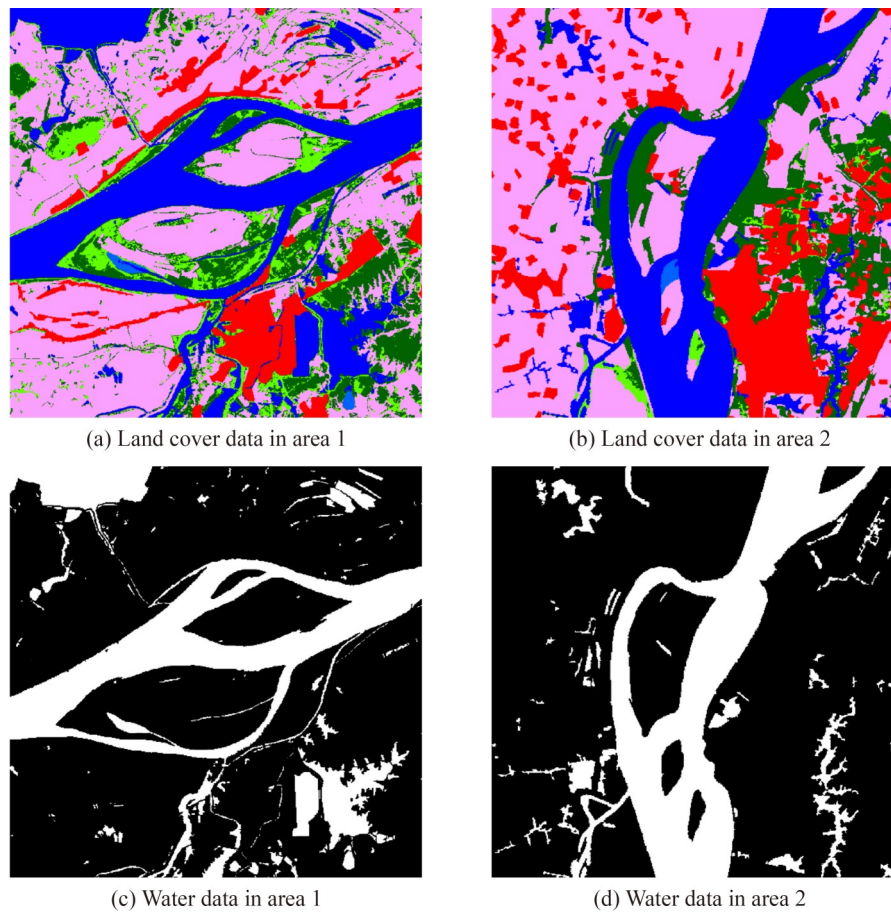


Figure 10 GIS data in the case

two areas and the start and target coordinates are shown in Table 3. Traditional APF algorithm and RRT algorithm were included in tests as a comparison. In addition, the basic parameters set for algorithms are shown in Table 4.

Table 3 The comparison of 2 areas in the case

Area	Length (km)	Test	Start (km)	Goal (km)	Distance (km)
Area 1	20	Test 1	(3, 14)	(25.4, 29.6)	27.297
		Test 2	(3, 15)	(27.6, 21.6)	25.470
		Test 3	(4, 16)	(34, 27.4)	32.093
		Test 4	(5, 14)	(28, 22.4)	24.486
Area 2	15	Test 5	(8.25, 1.125)	(7.875, 10.5)	9.382
		Test 6	(3.75, 1.95)	(9.75, 12)	11.705
		Test 7	(3.75, 1.95)	(6.375, 10.95)	9.375
		Test 8	(6.75, 0.75)	(10.5, 13.5)	13.290

5 Results

The results of eight path planning tests are illustrated in Figure 11, where black lines represent paths planned by

Table 4 The basic parameters setting

Parameter	Traditional APF	Improved APF	RRT
Iterations	10 000	10 000	10 000
Step-Size (unit)	5	5	5
α_0 (unit)	60	60	–
λ	1/500	1/500	–
n	–	100	–
β	–	1/2	–
μ	300	300	–

the improved APF algorithm, pink lines represent trajectories planned by the traditional APF algorithm, and blue lines represent paths estimated by the RRT algorithm. Since the RRT algorithm is not successfully planned the tree-like paths, paths planned by RRT algorithm are not shown in Figure 11(f) and Figure 11(g). The results indicate that the improved APF algorithm used in the case study achieved the desired trajectories. The improved APF algorithm achieved all planned paths to the goal successfully in eight tests, while the traditional APF algorithm achieved twice and the RRT algorithm achieved six tests. The traditional APF algorithm was trapped at the edge of huge obsta-

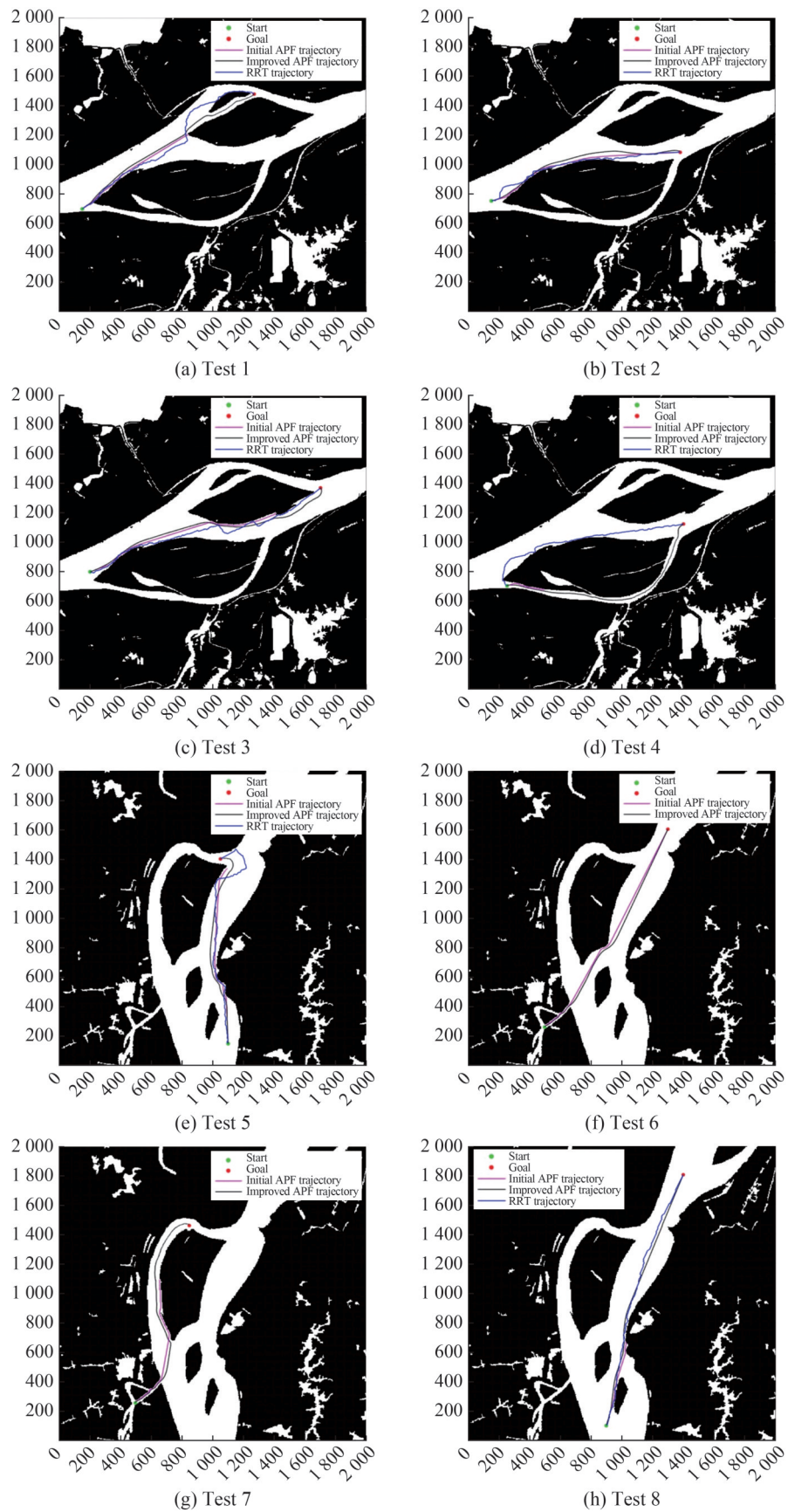


Figure 11 Planning path for tests

cles for tests 1, 4, 5 and 7. The improved APF algorithm enhanced the obstacle’s reach (as shown in Figure 8), which attenuated the influence of the obstacle edges and prevented the ERRVs from being only locally optimal at the obstacle edges. For tests 3 and 8, the traditional algorithm was stuck in the U-shaped obstacle region and could not proceed further. Virtual obstacles were set up and used to escape from the U-shaped region in the improved algorithm.

A comparison of the planned paths of tests 2 and 6 were shown in Figures 12 and 13 by calculating the curvatures of the entire paths. All algorithms were successful in providing the planned paths for test 2. Significantly, all APF algorithms planned smoother paths than RRTs, as shown in Figure 12(a), 13(a), and 13(b), which is consistent with Gu et al. (2023). Furthermore, a comparison of the two planned paths in tests 6 indicated that the paths estimated by the improved APF algorithm had the smallest curvature float range. The trajectory estimated by the traditional APF were affected by the irregular edges of the obstacles, which moved around the obstacles, as shown in Figure 12(b). The

improved APF algorithm suggested an optimized path to elude obstacles, resulting in smoother path. In test 6, the curvature of the initial APF trajectory was even above 1, while the curvature of the improved APF trajectory was always fluctuating around 0, as shown in Figures 13(c)–13(d).

The response time and number of iterations for both algorithms are described in Table 5. The results demonstrated that all APF algorithms performed more efficiently than the RRT algorithm significantly, which is consistent with Li et al. (2021). In test 2, the trajectory estimated by the improved APF algorithm was solved with 1 245 iterations, which was less than the traditional APF algorithm. This indicated that the relatively smoother path was solved by the improved algorithm in fewer steps. The response times of both APF algorithms were relatively close, but the time used by the improved APF algorithm (i.e., 8.38 s) was shorter than the traditional algorithm (i.e., 8.56 s). With the existing inland waterway GIS information, the improved APF algorithm responds quickly and successfully gives applicable paths for ERRVs.

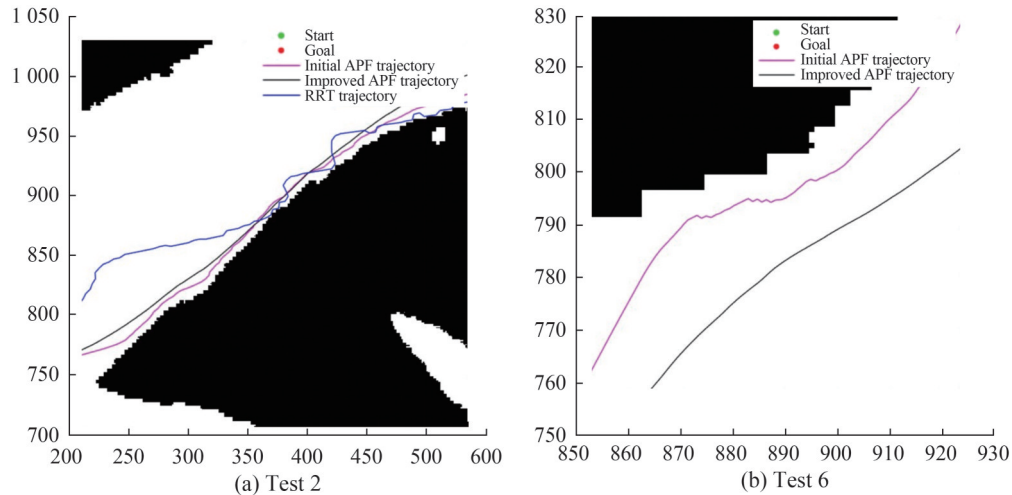


Figure 12 Localized enlarged view

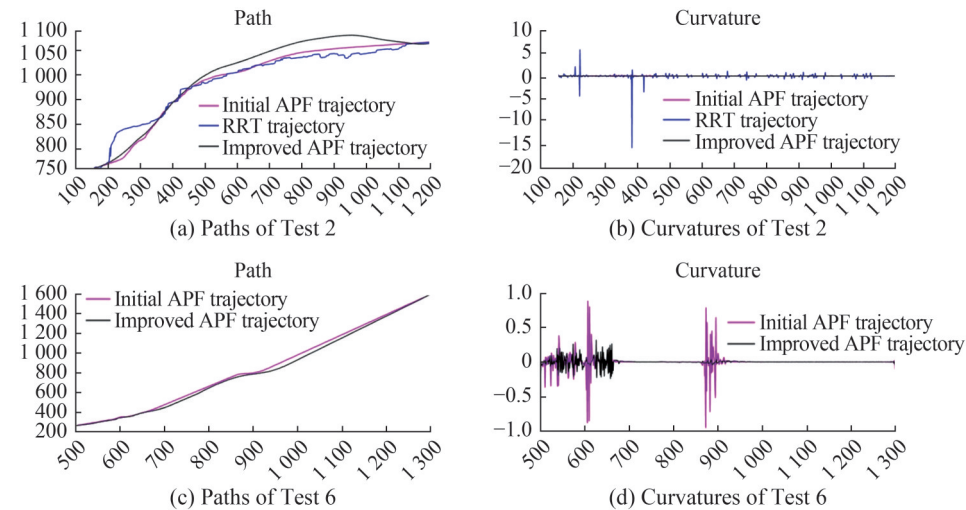


Figure 13 Curvature comparison

Table 5 Test results

Area	Test	Iterations			Time (s)		
		Traditional APF	Improved APF	RRT	Traditional APF	Improved APF	RRT
Area 1	Test 1	10 000	2 543	1 848	–	8.371 155	78.109 541
	Test 2	1 326	1 245	949	8.556 581	8.382 733	16.036 974
	Test 3	10 000	2 736	2 328	–	8.434 149	163.684 541
	Test 4	10 000	1 609	1 521	–	8.574 522	20.326 345
Area 2	Test 5	10 000	1 401	3 193	–	8.009 598	147.311 668
	Test 6	1 584	1 579	10 000	8.261 899	8.221 996	–
	Test 7	10 000	1 275	10 000	–	8.029 031	54.417 055
	Test 8	10 000	1 789	550	–	8.041 158	29.760 504

6 Discussion

The test results demonstrated that the traditional APF algorithm tended to be inadequate for path planning of the ERRV in a complex inland water environment, which was consistent with previous studies (Gan et al., 2022; Jadhav et al., 2023). There are many narrow channels in inland rivers that lead to failure of path planning, as shown in tests 4 and 7. When large obstacles and barriers appear, there is likely to be poor performance of the traditional APF algorithm (e.g., tests 1, 3, and 8). The improved APF algorithm was shown to achieve better performance than the traditional algorithm for the destination approach of the ERRV.

Besides destination approach, the improved APF algorithm was shown to be more efficient than the traditional APF algorithm in path planning of the ERRV. In the past, intelligent algorithms such as A* and RRT were often applied to avoid obstacles in planning appropriate path of different vehicles (Sang et al., 2021). The application of intelligent algorithms improves the overall search capability of the APF algorithm in a limited way but sacrifices the efficiency. In this study the proposed algorithm, based on the underlying layer of the algorithm, preserved the efficiency with fewer iterations and less response time (referred to Table 5).

To accommodate the dynamics of ERRVs, smooth paths are necessary. Instead of taking an additional curve fitting as most strategies do (Liu et al., 2024a), this study varies the gradient of the repulsive potential field to achieve a natural smooth path. In fact, additional fitting is necessary in the calculation process of some mainstream algorithms (e.g., RRT), because the generated paths are extremely convoluted. The proposed approach adds no extra computation, which increases algorithmic efficiency. The improved APF algorithm gave planning paths in only eight seconds when dealing with extreme maps with 4 000 000 units, which was only 0.05 time that of the RRT algorithm in some scenarios. It was shown that the improved APF algo-

rithm was capable of planning paths to nearly ten different targets every minute in a real rescue application.

The proposed path planning algorithm could be applied beyond ERRVs. The traditional APF algorithm is sensitive to the parameters, such as the gravitational parameter, the repulsive force parameter, and the radius of influence of the obstacle (Gu et al., 2023). The parameter variations induce changes to the properties of the algorithm (e.g., an increase in the radius of influence of obstacles leads to a path away from the obstacles). The improved APF algorithm retains the original parameters. Therefore, it is necessary to debug the parameters in advance in different application scenarios, which could improve the applicability and feasibility of the proposed method. For example, a more flexible path is possible for vessels with excellent mobility with small n .

7 Conclusion

In light of the growing occurrence of extreme weather events, inland water areas are suffering from frequent flood disasters. The ERRV is one of the most important approaches in ensuring life and property security. However, a complex inland river environment enhances the difficulty of ERRV path planning. This study thus proposes an improved APF algorithm to increase decision-making efficiency for path planning of ERRVs. A case study was conducted with an ERRV serving the water areas in the Yangtze River.

By conducting eight tests in two water areas in the Yangtze River, the improved algorithm was shown to be appropriate for inland river ERRV path planning. The results indicated that 1) the trajectories estimated by the improved APF algorithm successfully achieved the rescue goals in all tests, 2) the improved APF algorithm has high efficiency with fewer iterations and less response time, and 3) it achieved excellent smoothness.

Although this research obtained interesting results for

path planning of ERRVs, several limitations still exist. Only eight tests were carried out based on a simulation that had some discrepancy from the real situation. In future studies, an analysis of the proposed algorithm in large-scale scenarios would be valuable to increase the scalability to larger or more complex environments. It was assumed that the wave and the wind parameter were constant, which might be inappropriate to accurately reflect the dynamic conditions that ERRVs typically face. Thus, it is suggested that future studies conducting field experiments and real-world trials, especially in flooding disaster conditions, are necessary to capture the full complexity and unpredictability of real-world environments. In order to improve the robustness of the proposed algorithm, it is also expected to consider variable environmental factors such as fluctuating wind and wave conditions based on further real-world experiments. It is also suggested to compare the ERRV's paths planned by the proposed algorithm and the practical paths in realistic flooding disasters. Due to the parameter sensitivity of the proposed algorithm, a detailed parameter tuning strategy is recommended in future studies. It is recommended to further optimize the path planning algorithm in order to make it more compatible with the navigation of ERRVs in harsh environments.

Funding The National Natural Science Foundation of China (Grant No. 72274052), and the National Natural Science Foundation of China (Grant No. 72174173).

Competing interest The authors have no competing interests to declare that are relevant to the content of this article.

References

- Bolbot V, Theotokatos G, Boulougouris E, Vassalos D (2020) A novel cyber-risk assessment method for ship systems. *Saf. Sci.* 131: 104908. <https://doi.org/10.1016/j.ssci.2020.104908>
- Borowska-Stefańska M, Kowalski M, Wiśniewski S, Dulebenets MA (2023) The impact of self-evacuation from flood hazard areas on the equilibrium of the road transport. *Saf. Sci.* 157: 105934. <https://doi.org/10.1016/j.ssci.2022.105934>
- Cao S, Fan P, Yan T, Xie C, Deng J, Xu F, Shu Y (2022) Inland waterway ship path planning based on improved RRT algorithm. *J. Mar. Sci. Eng.* 10: 1460. <https://doi.org/10.3390/jmse10101460>
- Chi W, Ding Z, Wang J, Chen G, Sun L (2022) A generalized voronoi diagram-based efficient heuristic path planning method for RRTs in mobile robots. *IEEE Trans. Ind. Electron.* 69: 4926-4937 <https://doi.org/10.1109/TIE.2021.3078390>
- Fan K, Xu B (2023) The province's port and shipping resources integration reform landed five years-water transport Anhui to accelerate voyage. *Anhui News*
- Fazlollahab H (2018) Lagrangian relaxation method for optimizing delay of multiple autonomous guided vehicles. *Transp. Lett.* 10: 354-360. <https://doi.org/10.1080/19427867.2017.1386871>
- Gan L, Yan Z, Zhang L, Liu K, Zheng Y, Zhou C, Shu Y (2022) Ship path planning based on safety potential field in inland rivers. *Ocean Eng.* 260: 111928. <https://doi.org/10.1016/j.oceaneng.2022.111928>
- Gu Q, Zhen R, Liu J, Li C (2023) An improved RRT algorithm based on prior AIS information and DP compression for ship path planning. *Ocean Eng.* 279: 114595. <https://doi.org/10.1016/j.oceaneng.2023.114595>
- Hirabayashi Y, Mahendran R, Koirala S, Konoshima L, Yamazaki D, Watanabe S, Kim H, Kanae S (2013) Global flood risk under climate change. *Nat. Clim. Change* 3: 816-821. <https://doi.org/10.1038/nclimate1911>
- Jadhav AK, Pandi AR, Somayajula A (2023) Collision avoidance for autonomous surface vessels using novel artificial potential fields. *Ocean Eng.* 288: 116011. <https://doi.org/10.1016/j.oceaneng.2023.116011>
- Kellens W, Terpstra T, De Maeyer P (2013) Perception and communication of flood risks: a systematic review of empirical research. *Risk Anal.* 33: 24-49. <https://doi.org/10.1111/j.1539-6924.2012.01844.x>
- Khan AH, Li S, Chen D, Liao L (2020) Tracking control of redundant mobile manipulator: An RNN based metaheuristic approach. *Neurocomputing* 400: 272-284. <https://www.sciencedirect.com/science/article/pii/S092523122030343X>
- Khatib O (1985) Real-time obstacle avoidance for manipulators and mobile robots. *Proceedings of 1985 IEEE International Conference on Robotics and Automation* 500-505. <https://doi.org/10.1109/ROBOT.1985.1087247>
- Lan W, Jin X, Chang X, Zhou H (2024) Based on deep reinforcement learning to path planning in uncertain ocean currents for underwater gliders. *Ocean Eng.* 301: 117501. <https://doi.org/10.1016/j.oceaneng.2024.117501>
- Lavalle SM (1998) Rapidly-exploring random trees: a new tool for path planning. *The Annual Research Report*
- Li L, Wu D, Huang Y, Yuan ZM (2021) A path planning strategy unified with a COLREGS collision avoidance function based on deep reinforcement learning and artificial potential field. *Appl. Ocean Res.* 113: 102759. <https://doi.org/10.1016/j.apor.2021.102759>
- Li Z, Zhang X, Ma Y, Feng C, Hajiyev A (2019) A multi-criteria decision making method for urban flood resilience evaluation with hybrid uncertainties. *Int. J. Disaster Risk Reduct.* 36: 101140. <https://doi.org/10.1016/j.ijdrr.2019.101140>
- Liao B, Wan F, Hua Y, Ma R, Zhu S, Qing X (2021) F-RRT*: An improved path planning algorithm with improved initial solution and convergence rate. *Expert Syst. Appl.* 184: 115457. <https://doi.org/10.1016/j.eswa.2021.115457>
- Liu M, Zhang H, Yang J, Zhang T, Zhang C, Bo L (2024a) A path planning algorithm for three-dimensional collision avoidance based on potential field and B-spline boundary curve. *Aerosp. Sci. Technol.* 144: 108763. <https://doi.org/10.1016/j.ast.2023.108763>
- Liu Y, Chen C, Wang Y, Zhang T, Gong Y (2024b) A fast formation obstacle avoidance algorithm for clustered UAVs based on artificial potential field. *Aerosp. Sci. Technol.* 147: 108974. <https://doi.org/10.1016/j.ast.2024.108974>
- Liu Z (2021) China's port cargo throughput steadily ranked first in the world [Online]. *People's Daily*. https://www.gov.cn/xinwen/2021-10/04/content_5640899.htm [Accessed 3 April 2024]
- Liu Z, Cui J, Meng F, Xie H, Dan Y, Li B (2024c) Research on intelligent ship route planning based on the adaptive step size informed-RRT* algorithm. *J. Mar. Sci. Appl.* <https://doi.org/10.1007/s11804-024-00433-2>
- Lyridis DV (2021) An improved ant colony optimization algorithm for unmanned surface vehicle local path planning with multimodality constraints. *Ocean Eng.* 241: 109890. <https://doi.org/10.1016/j.oceaneng.2021.109890>

- Lyu H, Yin Y (2019) COLREGS-constrained real-time path planning for autonomous ships using modified artificial potential fields. *J. Navig.* 72: 588-608. <https://doi.org/10.1017/S0373463318000796>
- Ma Q, Zhou Y, Zhang M, Peng Q, Fu S, Lyu N (2023) A method for optimizing maritime emergency resource allocation in inland waterways. *Ocean Eng.* 289: 116224. <https://doi.org/10.1016/j.oceaneng.2023.116224>
- Ministry of Ecology and Environment of China (2022) Action Program for Deepening the Battle for the Protection and Restoration of the Yangtze River. https://www.mee.gov.cn/xxgk2018/xxgk/xxgk03/202209/t20220919_994278.html [Accessed 3 April 2024]
- Mizutori M, Guha-Sapir D (2020) The human cost of disasters: an overview of the last 20 years (2000–2019). Centre for Research on the Epidemiology of Disasters (CRED), United Nations Office for Disaster Risk Reduction
- National Geomatics Center of China (2024) *GlobeLand30 Data*. 2010 ed
- Ni S, Liu Z, Huang D, Cai Y, Wan, X, Gao S (2021) An application-orientated anti-collision path planning algorithm for unmanned surface vehicles. *Ocean Eng.* 235: 109298. <https://doi.org/10.1016/j.oceaneng.2021.109298>
- Ozkan MF, Carrillo LRG, King SA (2019) Rescue Boat Path Planning in Flooded Urban Environments. *IEEE International Symposium on Measurement and Control in Robotics (ISMCR)* 19-21. <https://doi.org/10.1109/ISMCR47492.2019.8955663>
- Paprotny D, Sebastian A, Morales-Nápoles O, Jonkman SN (2018) Trends in flood losses in Europe over the past 150 years. *Nat. Commun.* 9: 1985. <https://doi.org/10.1038/s41467-018-04253-1>
- Pehlivanoglu YV, Pehlivanoğlu P (2021) An enhanced genetic algorithm for path planning of autonomous UAV in target coverage problems. *Appl. Soft Comput.* 112: 107796. <https://doi.org/10.1016/j.asoc.2021.107796>
- Pinedo ML (2022) *Single Machine Models (Deterministic)*. In: PINEDO ML (ed.) *Scheduling: Theory, Algorithms, and Systems*. Cham: Springer International Publishing. https://doi.org/10.1007/978-3-031-05921-6_3
- Rao J, Xiang C, Xi J, Chen J, Lei J, Giernacki W, Liu M (2023) Path planning for dual UAVs cooperative suspension transport based on artificial potential field-A* algorithm. *Knowledge-Based Syst.* 277: 110797. <https://doi.org/10.1016/j.knsys.2023.110797>
- Rodríguez-Guerra D, Mosca A, Valente A, Cabanes I, Carpanzano E (2023) An advanced dual APF-based controller for efficient simultaneous collision and singularity avoidance for human-robot collaborative assembly processes. *CIRP Ann.* 72: 5-8. <https://doi.org/10.1016/j.cirp.2023.04.037>
- Roeleven D, Kokc M, Stipdonk HI, De Vries WA (1995) Inland waterway transport: Modelling the probability of accidents. *Saf. Sci.* 19: 191-202. [https://doi.org/10.1016/0925-7535\(94\)00020-4](https://doi.org/10.1016/0925-7535(94)00020-4)
- Sang H, You Y, Sun X, Zhou Y, Liu F (2021) The hybrid path planning algorithm based on improved A* and artificial potential field for unmanned surface vehicle formations. *Ocean Eng.* 223: 108709. <https://doi.org/10.1016/j.oceaneng.2021.108709>
- Silverman BW (1985) Some aspects of the spline smoothing approach to non-parametric regression curve fitting. *Journal of the Royal Statistical Society Series B-Methodological* 47: 1-21
- Sung I, Choi B, Nielsen P (2021) On the training of a neural network for online path planning with offline path planning algorithms. *Int. J. Inf. Manage.* 57: 102142. <https://doi.org/10.1016/j.ijinfomgt.2020.102142>
- Tu H, Deng Y, Li Q, Song M, Zheng X (2024) Improved RRT global path planning algorithm based on Bridge Test". *Rob. Auton. Syst.* 171: 104570. <https://doi.org/10.1016/j.robot.2023.104570>
- Wang H, Fu Z, Zhou J, Fu M, Ruan L (2021a) Cooperative collision avoidance for unmanned surface vehicles based on improved genetic algorithm. *Ocean Eng.* 222: 108612. <https://doi.org/10.1016/j.oceaneng.2021.108612>
- Wang Z, Li G, Ren J (2021b) Dynamic path planning for unmanned surface vehicle in complex offshore areas based on hybrid algorithm. *Comput. Commun.* 166: 49-56. <https://doi.org/10.1016/j.comcom.2020.11.012>
- Xiong W, Gelder P, Yang K (2020) A decision support method for design and operationalization of search and rescue in maritime emergency". *Ocean Eng.* 207: 107399. <https://www.sciencedirect.com/science/article/pii/S0029801820304285>. <https://doi.org/10.1016/j.oceaneng.2020.107399>
- Ye L, Wu F, Zou X, Li J (2023) Path planning for mobile robots in unstructured orchard environments: An improved kinematically constrained bi-directional RRT approach. *Comput. Electron. Agric.* 215: 108453. <https://doi.org/10.1016/j.compag.2023.108453>
- Yu J, Chen C, Arab A, Yi J, Pei X, Guo X (2024) RDT-RRT: Real-time double-tree rapidly-exploring random tree path planning for autonomous vehicles. *Expert Syst. Appl.* 240: 122510. <https://doi.org/10.1016/j.eswa.2023.122510>
- Zhai Y, Cui J, Meng F, Xie H, Hou C, Li B (2024) Ship path planning based on sparse A* algorithm. *J. Mar. Sci. Appl.* <https://doi.org/10.1007/s11804-024-00430-5>
- Zhang L, Mou J, Chen P, Li M (2021) Path planning for autonomous ships: a hybrid approach based on improved APF and modified VO methods. *J. Mar. Sci. Eng.* 9: 761. <https://doi.org/10.3390/jmse9070761>
- Zhou L, Kong M (2022) 3D obstacle-avoidance for a unmanned aerial vehicle based on the improved artificial potential field method. *Journal of East China Normal University (Natural Science)* 2022: 54-67. <https://doi.org/10.3969/j.issn.1000-5641.2022.06.007>